Fırat Üniversitesi Deneysel ve Hesaplamalı Mühendislik Dergisi

FUJECE

Makine Öğrenmesi Tabanlı Regresyon Metotları ile Üç Boyutlu (3B) Baskı Parça Kalitesinin Tahmini

Ahmet Burak TATAR[1]*

[1]Mekatronik Mühendisliği, Mühendislik Fakültesi, Fırat Üniversitesi, Elazığ, Türkiye.
[1]atatar@firat.edu.tr

Geliş Tarihi: 19.12.2024
Kabul Tarihi: 30.01.2025

Düzeltme Tarihi: 26.12.2024

doi: https://doi.org/10.62520/fujece.1604379
Araştırma Makalesi

Alıntı: A.B. Tatar, "Makine öğrenmesi tabanlı regresyon metotları ile üç boyutlu (3b) baskı parça kalitesinin tahmini", Fırat Üni. Deny. ve Hes. Müh. Derg., vol. 4, no 1, pp. 206-225, Şubat 2025.

Öz

Bu çalışmada farklı alanlarda kullanılacak ürünlerin üç boyutlu yazıcılarda imal edilirken baskı parametreleri dikkate alınarak kullanım amacına göre parçanın pürüzlülük oranı, yüke dayanımı ve çekme kuvvetine göre uzama gerilmesi verileri değerlendirilmiş ve ürün kalitesi makine öğrenmesi regresyon metotları ile optimize edilmiştir. Ürün kalitesinin tahmini için Kaggle platformundan elde edilen "3D Printer Material Requirement" açık kaynak veri seti kullanılmıştır. Bu veri setinde sisteme girdi olarak verilen; katman yüksekliği, duvar kalınlığı, dolgu yoğunluğu, dolgu deseni, nozul sıcaklığı, tabla (yatak) sıcaklığı, baskı hızı, baskı malzemesi (PLA ve ABS) ve fan hızı parametrelerine göre baskı sonucu ürünün pürüzlülüğü, yüke dayanım gücü ve çekme kuvvetlerinin etkisiyle ürünün uzama gerilmesi değerleri incelenmiştir. Bu değerler doğrultusunda da ürünün kullanım amacına göre kalitesi tahmin edilmeye çalışılmıştır. Katman yüksekliği, duvar kalınlığı, dolgu yoğunluğu, dolgu deseni, nozul sıcaklığı, yatak sıcaklığı, baskı hızı, baskı malzemesi ve fan hızı gibi parametreler, çıktı performansını etkileyen temel faktörler olarak kullanılmıştır. Bu çerçevede, Linear Regression (LR), Decision Tree (DT), Random Forest (RF), Support Vector Machine (SVM), Gaussian Process Regression (GPR), Multi-Layer Perceptron (MLP) tahmin modelleri geliştirilmiş ve model performansları, doğruluk (R^2), hata oranları (RMSE, MSE, MAE) ve işlem süresi gibi metrikler açısından değerlendirilmiştir. Bu yöntemler içerisinde GPR ile uzanım, gerilim mukavemeti ve pürüzlülük açısından en başarılı tahmin oranları sırasıyla 0,98, 0,9 ve 1 olarak elde edilmiştir. Elde edilen bulgular, 3B yazıcıların üretim süreçlerinde kalite tahmini ve optimizasyonu için makine öğrenmesi uygulamalarının etkili bir araç olduğunu göstermektedir. Ayrıca bu çalışma, 3B baskı süreçlerinde kalite kontrolü ve tasarım optimizasyonuna yeni bir perspektif sunmaktadır.

Anahtar kelimeler: 3D baskı, Makine öğrenmesi, Regresyon, Baskı parametreleri

*Yazışılan Yazar

İntihal Kontrol: Evet – Turnitin
Şikayet: fujece@firat.edu.tr

Firat University Journal of Experimental and Computational Engineering

Predicting Three-Dimensional (3D) Printing Product Quality with Machine Learning-Based Regression Methods

Ahmet Burak TATAR[1]*

[1]Mechatronics Engineering, Faculty of Engineering, Fırat University, Elazığ, Türkiye.
[1]atatar@firat.edu.tr

Received: 19.12.2024
Accepted: 30.01.2025
Revision: 26.12.2024
doi: https://doi.org/10.62520/fujece.1604379
Research Article

Citation: A.B. Tatar, "Predicting Three-Dimensional (3D) Printing Product Quality with Machine Learning-Based Regression Methods", Firat Univ. Jour.of Exper. and Comp. Eng.., vol. 4, no 1, pp. 206-225, February 2025.

Abstract

This study examines how printing parameters affect the roughness, tensile strength, and elongation of 3D-printed parts used in various applications. Machine learning-based regression models were employed to optimize product quality. The open-source "3D Printer Material Requirement" dataset obtained from the Kaggle platform was utilized to predict product quality. This dataset includes input parameters such as layer height, wall thickness, infill density, infill pattern, nozzle temperature, bed temperature, print speed, printing material (PLA and ABS), and fan speed. These parameters were analyzed for their impact on the product's roughness, load resistance, and elongation under tensile force. Based on these evaluations, product quality was estimated according to its intended use. Parameters such as layer height, wall thickness, infill density, infill pattern, nozzle temperature, bed temperature, print speed, printing material, and fan speed were identified as key factors influencing output performance. Within this framework, prediction models including Linear Regression (LR), Decision Tree (DT), Random Forest (RF), Support Vector Machine (SVM), Gaussian Process Regression (GPR), and Multi-Layer Perceptron (MLP) were developed, and their performances were assessed using metrics such as accuracy (R^2), error rates (RMSE, MSE, MAE), and computational time. Among these methods, GPR demonstrated the highest prediction accuracy for elongation, tensile strength, and roughness, with respective values of 0.98, 0.9, and 1. The findings indicate that machine learning applications are effective tools for quality prediction and optimization in the production processes of 3D printers. Furthermore, this study provides a novel perspective on quality control and design optimization in 3D printing processes.

Keywords: 3D printing, Machine learning, Regression, Printing parameters.

*Corresponding Author

1. Introduction

3D printing is an additive manufacturing process that creates physical three-dimensional objects from digital models by depositing materials layer by layer, offering advantages over traditional subtractive manufacturing methods [1]. Today, 3D printing has revolutionized design and manufacturing by enabling rapid prototyping, producing intricate geometries, and facilitating cost-effective small-scale production. This technology is widely adopted in both industrial and personal applications. The technology plays a significant role in areas such as prototype production, medical devices, and aerospace applications. However, the multitude of parameters influencing the quality of 3D-printed parts complicates process optimization. The printing process involves parameters that can impact print quality, microstructure, and certain properties [2]. These properties can be enhanced through the optimization of parameters such as layer height, infill density, nozzle temperature, and print speed. Nevertheless, traditional experimental approaches to understanding these parameters' effects are often time-consuming and costly. Machine learning algorithms, by analyzing multidimensional and complex datasets, offer the potential to predict these effects quickly and effectively.

The integration of data-driven artificial intelligence and its subset, machine learning (ML), accelerates the optimization of 3D printing parameter settings while reducing time and cost [3]. Recent advances in ML have opened new avenues to address these challenges. ML algorithms can uncover complex relationships between input parameters and output quality metrics, enabling more accurate predictions and optimizations. Leveraging these capabilities, this study aims to develop a predictive framework for 3D-printed part quality and reduce reliance on experimental trial-and-error methods.

This study utilizes the "3D-Printer Material Requirement" dataset available on Kaggle [4] to predict 3D printing part quality through machine learning-based regression methods. The results provide detailed insights into the effects of printing parameters on part quality and offer actionable outputs for quality optimization. Parameters such as layer height, wall thickness, infill density, infill pattern, nozzle temperature, bed temperature, print speed, printing material (PLA and ABS), and fan speed were analyzed for their effects on surface roughness, tensile strength, and elongation at break of the printed parts.

Optimizing these parameters to enhance product performance not only ensures material savings but also enables the production of higher-quality outputs. In addition, this study will ensure that the product to be printed on the 3D printer is manufactured with optimum accuracy according to its intended use. For example, a spur gearbox mechanical part that is expected to be resistant to loads and tensile forces that may occur, or a figurine that is constantly in a static state and is not exposed to any load but is expected to have minimum roughness and can be used as an ornament, will be obtained with optimum printing.

In this paper; Chapter 2 includes a literature review in which similar studies on the subject are researched and presented. Chapter 3 provides the contributions of this study to the literature and the originality of the study. Chapter 4 presents the materials and methods required for the implementation of this study. Chapter 5 provides experimental results as a result of the study and evaluates these results. Chapter 6 includes the evaluation of the success of the study according to the results obtained and its interpretation and conclusion.

2. Literature Review

The manufacturing of parts using 3D printing techniques and products (Figure 1) is widely applied for various purposes, including robotic applications [5-7], healthcare services [8-10], space exploration [11], aviation [12], mechanical fasteners [13], and diverse products offering practical solutions for everyday life [14]. These parts, whether designed to operate under static and dynamic loads or to perform tasks without being subjected to any loads, must be manufactured with high quality according to their intended use by employing the correct method and appropriate printing parameters. Therefore, optimizing product quality based on the intended application through different 3D printing parameters ensures the successful completion of the manufacturing process.

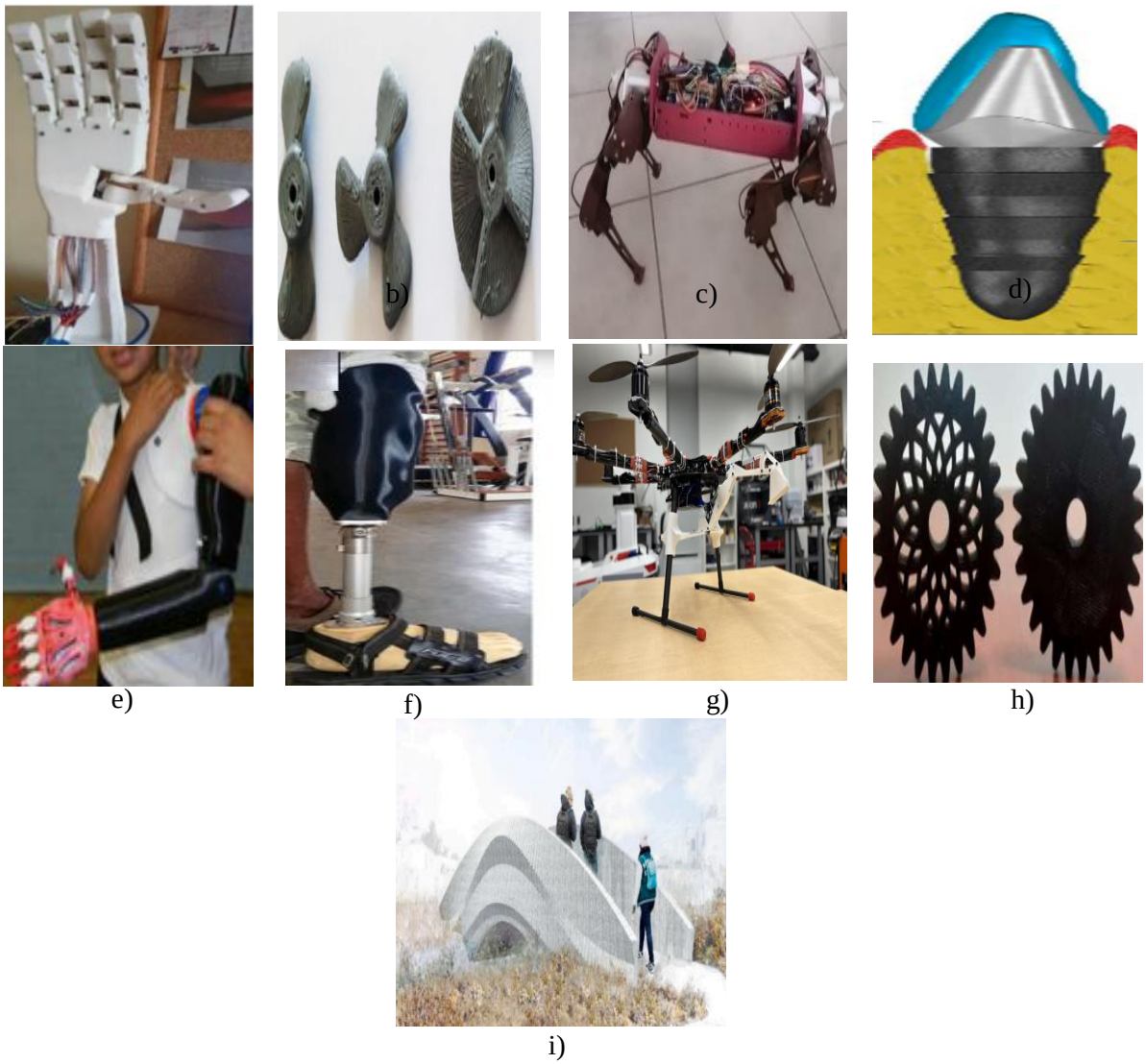

Figure 1. Examples of 3D-printed products; **a)** Prosthetic hand [5], **b)** Propeller [6], **c)** Quadruped robot [7], **d)** Dental implant [8], **e)** Prosthetic arm [9], **f)** Prothetic leg [10], **g)** Drone [11], **h)** Spur gear [12], **i)** 3D-printed bridge [13]

Artificial intelligence algorithms can be leveraged to predict the quality of parts produced through 3D printing. By evaluating the effects of printing parameters on the output product, it becomes possible to optimize part quality. Recent studies have demonstrated the effectiveness of machine learning in optimizing 3D printing parameters [15-22, 27];

Omigdobun et al. [15] developed a predictive framework employing multiple machine learning regression algorithms to enhance the mechanical and thermal properties of PLA, a 3D printing material, for biomedical applications. They achieved high prediction accuracies, with R^2 metrics of 0.9173 and 0.8772 for compressive and tensile strengths, respectively. Kasim et al. [16] investigated the influence of infill density and print speed on the microstructure and tensile behavior of 3D-printed parts. Their results indicated that maintaining a print speed below the threshold of 40 mm/s positively impacts product quality, while higher infill percentages enhance the part's strength.

Zhang et al. [17] optimized the dynamic performance of 3D-printed spur gears using a Genetic Algorithm-based Artificial Neural Network for multi-parametric regression. By analyzing parameters such as nozzle temperature, print speed, bed temperature, and infill percentage, they concluded that wear performance improved threefold. Pereira et al. [18] evaluated parts produced with varying layer thickness, print speed, infill density, infill pattern, and material parameters through tensile, compression, and bending mechanical

tests. Their optimization aimed to minimize time and total weight, resulting in a 72.39% reduction in print time and a 9.06% increase in mass.

Sani et al. [19] emphasized the potential of Artificial Intelligence-Augmented Additive Manufacturing (AI2AM) technology in detecting defects, improving production quality, and minimizing risks of failure. The AI2AM framework proved effective in optimizing printer operations under ideal conditions. Sevli [20] focused on material selection for 3D printing using machine learning methods. By evaluating the impact of different materials on print parameters and outcomes, the study proposed a model for optimal material selection, achieving 100% accuracy in classification using the Logistic Regression algorithm.

Dabbagh et al. [21] employed Gradient Boosting Regression (GBR) to determine the optimum printing parameters for manufactured parts, achieving a prediction accuracy with an R^2 score of 0.954. Similarly, Jatti et al. [22] used a machine learning regression model to predict tensile, impact, and bending test outcomes for printed parts, achieving lower percentage errors of 3.109, 6.532, and 3.712, respectively.

Nair et al. [27], in a study similar to this one, performed the prediction of 3D model selection using various machine learning methods and evaluated the processes of elongation, roughness, and tensile strength. The success evaluation of the results they obtained has been compared with the success rates in the results section of this study.

These studies demonstrate the growing role of machine learning in enhancing the quality and efficiency of 3D printing, paving the way for advanced manufacturing solutions.

3. Contribution and Novelty

This study offers a novel perspective on the application of machine learning algorithms in 3D printing processes. The multidimensional structure of the dataset highlights the interactions among multiple printing parameters, enabling a deeper understanding of their effects on print quality. By comparing the performance of different regression models, the study identifies the most suitable algorithm, providing valuable contributions to both academic literature and industrial applications. The application of machine learning techniques, particularly regression methods, to predict 3D printer quality constitutes a noteworthy methodological contribution. Unlike traditional analytical methods, these models enable the modeling of more complex relationships and generate actionable predictions.

The proposed model captures the nonlinear effects of parameters, facilitating accurate adjustments to printer settings and improving quality in the production process. This is particularly advantageous for rapid prototyping, small-batch production, and personal manufacturing processes, yielding significant time and cost savings. Moreover, the study can serve as a decision-support tool for 3D printer users, assisting them in optimizing parameters ranging from material selection to print speed, thereby enhancing the overall printing experience and outcomes.

4. Material and Method

4.1. Feature of 3D printer dataset

In this study we used an open access dataset, which publish in kaggle platform (3D Printer Material Requirement- https://www.kaggle.com/datasets/shubhamgupta012/3d-printer-material-requirement) [4]. This dataset provides comprehensive information on various parameters and properties involved in the 3D printing process. It includes data on factors such as layer thickness, wall width, infill density, infill pattern, nozzle temperature, bed temperature, printing speed, material type, fan speed, surface roughness, tensile strength, and elongation. These variables are critical elements that can influence the quality, durability, and aesthetic appearance of 3D-printed objects. Researchers can analyze this dataset to understand how different printing parameters affect the final output. The data can be utilized to explore correlations between printing settings and the physical properties of printed objects, optimize printing conditions, and identify new trends in 3D printing techniques. The primary goal of this dataset is to facilitate the analysis and experimentation of

3D printing processes, enabling users to make informed decisions about printing settings to achieve desired results.

4.2. Regression analysis based machine learning methods

4.2.1. Multiple linear regression model

In the multiple linear regression model, the dependent variable y is predicted based on multiple independent variables (x_1, x_2, x_3 ... x_p) Each of these independent variables is included in the model with a separate coefficient to explain its effect on the dependent variable. The general equation of the model is as follows [23]:

$$y = b_0 + b_1x_1 + b_2x_2 + \cdots + b_px_p + \epsilon \quad (1)$$

y is the dependent target variable, , x_1, x_2, x_3 ... x_p are the independent input variables, b_0 is the intercept term, b_1, b_2 , b_3 …. $b_n$are the coefficients of each independent variable, and ϵ represents the error term. The objective is to determine the coefficients (b_0 , b_1, b_2 …. b_n) that best predict the dependent variable yyy. In multiple regression, the coefficients (b_0 , b_1, b_2 …. b_n) are estimated using the Ordinary Least Squares (OLS) method, as shown in Equation (2). The Residual Sum of Squares (RSS) cost function, defined in Equation (3), is minimized to calculate these coefficients.

$$\mathrm{b} = (\mathrm{X}^T\mathrm{X})^{-1}\mathrm{X}^T\mathrm{y} \quad (2)$$
$$RSS = \text{Minimize} \sum_{i=1}^{n} (y_i - \hat{y}_i)^2 \quad (3)$$

4.2.2. Decision tree regression model

The Decision Tree Regression Model is a widely used non-linear predictive modeling method valued for its interpretability and ability to manage both numerical and categorical data effectively. In this study, the Decision Tree algorithm [24] was applied to evaluate its performance in predicting target variables such as roughness, tensile strength, and elongation, using independent variables including layer height, wall thickness, infill density, nozzle temperature, bed temperature, print speed, and fan speed.

The model operates by iteratively dividing the dataset into smaller subsets based on feature values, resulting in a tree-like structure. At each decision point, the algorithm identifies the feature and threshold that minimize the variance within the resulting partitions. This splitting process continues until predefined conditions, such as maximum tree depth or a minimum number of samples per leaf, are met. The predicted value for each terminal node is the mean value of the target variable for the data points in that subset.

In this study, hyperparameters like maximum tree depth and minimum samples per split were fine-tuned to balance prediction accuracy and prevent overfitting. The Decision Tree Regression Model effectively captured non-linear relationships between the independent variables and the target outcomes, providing valuable insights into the factors significantly influencing roughness, tensile strength, and elongation.

4.2.3. Random forest regression model

The Random Forest (RF) regression technique constructs an ensemble of decision trees to perform regression tasks. In this approach, multiple regression trees are generated, and their predictions are combined to produce a final result, typically by averaging their outputs [25]. This method operates by recursively dividing the input data into subsets through binary splits, creating a hierarchical structure resembling a forest. At each split, the algorithm identifies the feature and threshold that best separate the data into smaller, more homogeneous groups. This process minimizes the sum of squared deviations within the resulting partitions [25]. The regression tree algorithm focuses on optimizing the partitioning at each node by solving the following minimization problem :

$$arg\,min[P_l Var(Y_l) + P_r Var(Y_r)] \qquad x_j = x_j^R, j = 1,2,3 \ldots, M \tag{4}$$

In Eq. (4), P_l and P_r resent the probabilities of the left and right child nodes, respectively. M denotes the total number of features in the dataset. X_j and x_j^R indicate the feature and its optimal split point. $Var(Y_l)$, $Var(Y_r)$ correspond to the variance of the target variable in the left and right child nodes. The algorithm seeks to achieve the optimal split by minimizing the weighted variance of the target variable across the two partitions. This approach is notably robust to outliers and variations in the dataset, making it effective for regression tasks where data quality may vary. By leveraging the strengths of multiple decision trees, Random Forest regression provides a more stable and reliable prediction compared to individual regression trees.

4.2.4. Supported vector machine regression model

Support Vector Machines (SVMs) are supervised learning methods applied to both classification and regression problems [20]. When adapted for regression tasks, the dataset can be represented as [24]:

$$D = \{(x_1, y_1), (x_2, y_2), \ldots, (x_l, y_l)\} \tag{5}$$

Here, x_i represents the N-dimensional input features, and y_i denotes the corresponding output variable. The regression function is defined as:

$$f(x) = \langle w, x \rangle + b \tag{6}$$

n this equation, www is the weight vector (also known as the normal vector), x is the input vector, and b is the bias term. The dot product w, x ensures that the inputs and weights are isodimensional. The goal in Support Vector Regression (SVR) is to determine a function $f(x)$ that estimates the output values y_i with a maximum allowable deviation ϵ, while minimizing the distance between two parallel planes surrounding the data. To achieve this, the optimization problem involves minimizing the norm of the vector w, formulated as:

$$min\frac{1}{2}\|w\|^2 + C\sum_{i-1}^{l}(\xi_i + \xi_i^*) \tag{7}$$
$$y_i - \langle w, x_i \rangle - b \leq \varepsilon + \xi_i \tag{8}$$
$$\langle w, x_i \rangle + b - y_i \leq \varepsilon + \xi_i^* \tag{9}$$
$$\xi_i, \xi_i^* \geq 0 \tag{10}$$

Here, ξ_i, ξ_i^* are slack variables that allow deviations beyond ϵ. C is a regularization constant greater than 0, balancing the trade-off between the model's complexity and the tolerance for errors. Compared to traditional neural network-based supervised learning methods, SVMR employs the principle of **structural risk minimization**. This approach not only minimizes the empirical error (training error) but also reduces the generalization error's upper bound, making the model robust and effective for unseen data.

4.2.5. Gaussian process regression (GPR)

Gaussian Process Regression (GPR) is a non-parametric machine learning technique designed to predict the values of continuous response variables. This method models the output variable as a Gaussian process by establishing covariance relationships with the input features. A key advantage of GPR lies in its flexibility, as it offers a range of covariance (kernel) functions, enabling the selection of the most appropriate function for the specific problem at hand. This adaptability allows the creation of models capable of capturing relationships of varying complexity. A Gaussian process extends the Gaussian distribution concept from random variables to functions. While a Gaussian distribution describes the distribution of random values, a Gaussian process represents the distribution over functions. The Gaussian process function $f(x)$ is defined using a mean function $m(x)$ and a covariance function $k(x, x')$ as shown below [26]:

$$m(x) = E(f(x)) \tag{11}$$

$$k(x, x') = E(f(x) - m(x))(f(x') - m(x'))) \quad (12)$$

Here, , $k(x, x')$ represents the kernel or covariance function that describes the relationship between different points in the input space. The function (x) can be expressed as:

$$f(x) = GP(m(x), k(x. x')) \quad (13)$$

Typically, the mean function $m(x)$, is assumed to be zero for simplification. The relationship between the input vector x_i and the output variable y_i in GPR can be described as:

$$y_i = f(x_i) + \varepsilon \quad (14)$$

In this equation, $f(x)$ represents the regression function, while ϵ denotes the noise term, typically modeled as Gaussian noise. The covariance matrix for the Gaussian process is defined by $k_{i,j}$ which specifies the covariance between two points $f(xi)$ and $f(xj)$.in the input space as Eq.(15). The covariance matrix can be represented as Eq.(16)

$$k_{i,j} = k(x_i, x_j) \quad (15)$$

$$k = \begin{pmatrix} k(x_1, x_1) & k(x_1, x_2) & k(x_1, x_n) \\ \vdots & \vdots & \vdots \\ k(x_n, x_1) & \dots & k(x_n, x_n) \end{pmatrix} \quad (16)$$

This covariance structure allows GPR to capture the relationships between inputs, making it a robust approach for modeling complex patterns in data. By leveraging this framework, GPR can provide accurate predictions while accounting for uncertainty in the data.

4.2.6. Multi-layer perceptron regression model

The MLP (Multi-Layer Perceptron) regression model is an artificial neural network model designed to predict a numerical target value by working through multiple layers of nonlinear transformations from input to output. The independent variables in the model's input are represented by the vector $\mathbf{x} = [x_1, x_2, \dots, x_d]^T$, and this vector is passed to the first hidden layer. At each hidden layer, the following transformation is performed [24]:

$$\mathbf{z}^{(l)} = g\left(\mathbf{W}^{(l)} \cdot \mathbf{z}^{(l-1)} + \mathbf{b}^{(l)}\right) \quad (17)$$

Here: *l*, layer number, z(l−1) is the output of the previous layer. W(l), Weight matrix of *l*-th layer, b(l), The bias vector of the l-th layer, g is the activation function (ReLU, Sigmoid, Tanh, vb.). While activation functions are generally used to add nonlinearity in hidden layers, activation function is generally not applied in the output layer because of the regression problem. The output is;

$$\hat{y} = \mathbf{W}^{(o)} \cdot \mathbf{z}^{(L)} + \mathbf{b}^{(o)} \quad (18)$$

.

$\mathbf{W}^{(o)}$, is the weight vector from the last hidden layer to the output layer, $\mathbf{b}^{(o)}$ bias term of the output layer, $\mathbf{z}^{(L)}$ is the output of the last hidden layer. A loss function is defined based on the difference between the model's prediction and the actual values. N, total number of data, y_i actual target value, $\hat{y}_i$, is the model's predicted value.

$$L = \frac{1}{N}\sum_{i=1}^{N} (\hat{y}_i - y_i)^2 \quad (19)$$

Model weights and bias values are optimized via derivatives of the loss function. $\delta^{(o)}$, represents the error signal in the output layer. The error signal in the hidden layers is calculated by the chain rule, the learning rate is η. $g'(\mathbf{z}^{(l)})$ is the derivative of the activation function. $\odot$ expresses element-wise multiplication.

$$\delta^{(o)} = \hat{y} - y \tag{20}$$
$$\delta^{(l)} = \left(\mathbf{W}^{(l+1)}\right)^{\top} \delta^{(l+1)} \odot g'(\mathbf{z}^{(l)}) \tag{21}$$
$$\mathbf{W}^{(l)} = \mathbf{W}^{(l)} - \eta \cdot \delta^{(l)} \cdot \left(\mathbf{z}^{(l-1)}\right)^{\top} \tag{22}$$
$$\mathbf{b}^{(l)} = \mathbf{b}^{(l)} - \eta \cdot \delta^{(l)} \tag{23}$$

4.3. Selected parameters of ML methods

In this study, the dataset was evaluated using 10-fold cross-validation to ensure robust training and testing. This method splits the data into 10 equal parts, using 9 folds for training and 1 fold for testing iteratively, thus maximizing the use of the dataset while minimizing bias and variance in performance evaluation. The parameters employed in the regression models are detailed in Table 1, showcasing the specific configurations used for each model. This approach ensures a comprehensive and fair comparison of model performance across varying conditions.

Table 1. Parameter of used regression models

Multiple Linear Regression (MLR)	Preset: Robust Linear Term: Linear Robust option: On
Decision Tree (DT)	Preset: Fine Min. leaf size:4 Surrogate dessicion splits: Off
Random Forest (RF)	Preset: Boosted Trees Min. leaf size:8 Number of leraners:30 Learning rate:0.1
Support Vector Machine (SVM)	Preset: Cubic Kernel function: Cubic Kernel scale: Auto Box constraint: Auto Epsilon:Automatic Standardize data: True
Gaussian Process Regression (GPR)	Preset: Exponential GPR Basis function: Constant Kernel function: Squared Exponential Use Isoterapic kernel true Kernel scale: Automatic Signal standard deviation: Automatic Sigma: Automatic Standardize: True Optimize numeric parameters: True
Multi-Layer Perceptron Regression (MLP)	Preset: Medium Number of fully connecte layer: 1 First layer size: 25 Activation: ReLu Iteration limit:1000 Regularization streght: 0 Standardize data: True

4.4. Performance evaluation metrics

In this study, the performance of the regression models was assessed using six metrics, which are essential for evaluating the models' accuracy and generalizability. To determine performance, the

regression coefficient (R^2), mean absolute error (MAE), mean squared error (MSE), and root mean squared error (RMSE) were calculated. These metrics are described mathematically as Eq. (24-27).

$$MAE = \frac{1}{n}\sum_{i=1}^{n}|y_i - \hat{y}_i| \tag{24}$$

This metric calculates the average of the absolute differences between actual (y_i) and predicted ($\hat{y}_i$) values. A low MAE indicates that the model's predictions closely match the actual values.

$$MSE = \frac{1}{n}\sum_{i=1}^{n}(y_i - \hat{y}_i)^2 \tag{25}$$

This metric takes the average of the squared differences between actual and predicted values, giving greater weight to larger errors. A lower MSE indicates higher model accuracy.

$$RMSE = \sqrt{\frac{1}{n}\sum_{i=1}^{n}(y_i - \hat{y}_i)^2} \tag{26}$$

The RMSE provides the average size of prediction errors in the original measurement units. A low RMSE suggests that the model makes precise predictions.

$$R^2 - \frac{\sum(y_i - \hat{y}_i)^2}{\sum(y_i - \bar{y})^2} \tag{27}$$

This metric explains the proportion of variability in the dataset accounted for by the model. Values close to 1 indicate that the model has high explanatory power, effectively capturing the patterns in the data. *N* is the number of samples, $\hat{y}$ is predicted value of y, $\bar{y}$ is mean of experimental results of y.

5. Experimental Results and Discussion

In this study, all solutions were tested on a workstation with an Intel Core i7-9700K, RAM: 16 GB DDR4, GPU: NVIDIA GTX 1660 Ti and 64-bit Windows 11 Pro features. MATLAB 2023a version was used for all applications within the scope of the study.

5.1. Description of the datasets

The characteristics of the dataset are illustrated in Figure 2. The horizontal line connected to the dashed line represents the minimum and maximum values within the dataset. The blue box indicates the interquartile range, with its upper and lower boundaries corresponding to the 75th and 25th percentiles, respectively. Additionally, outliers are depicted as small circular markers positioned outside the minimum and maximum distribution, highlighting data points that deviate significantly from the central range. This visualization provides a comprehensive overview of the dataset's spread, variability, and outlier presence.

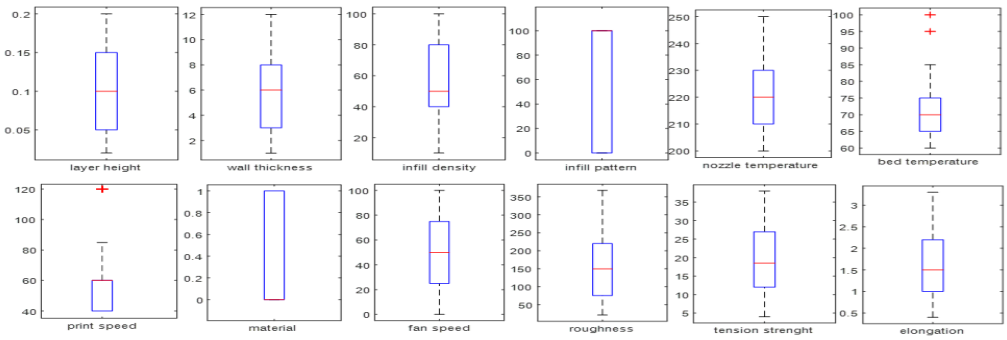

Figure 2. The analysis of the variables

In Table 2, specific statistical parameters have been calculated and presented for a comprehensive analysis of the dataset. Parameters such as layer height and wall thickness exhibit relatively homogeneous distributions, with low standard deviations (0.0626 and 2.95, respectively). In contrast, parameters like infill density and fan speed show higher standard deviations (27.55% and 35.83%, respectively), reflecting a wider variation. This indicates that some parameters were optimized within specific limits, while others were tested across a broader range. Nozzle temperature and bed temperature exhibit controlled variations, with standard deviations of 15.09 and 8.65, respectively, suggesting that these parameters were adjusted according to material compatibility. Regarding outputs, roughness (standard deviation 95.70) and tensile strength (standard deviation 9.20) demonstrate significant variability, indicating differences in mechanical performance and surface quality. On the other hand, elongation values vary within a narrower range (standard deviation 0.76), indicating more consistent results in terms of flexibility.

Table 2. Statistical analysis of the dataset

Feature	**Count**	**Mean**	**Std**	**Min**	**25%**	**50%**	**75%**	**Max**
Layer Height	132	0,098182	0,062608	0,02	0,0525	0,1	0,15	0,2
Wall Thickness	132	5,583333	2,952943	1	3	6	8	12
Infill Density	132	54,72727	27,54551	10	40	50	80	100
Nozzle Temperature	132	222,2727	15,09411	200	210	220	230	250
Bed Temperature	132	70,37879	8,651839	60	65	70	75	100
Print Speed	132	64,24242	28,59858	40	40	60	60	120
Fan Speed	132	48,5303	35,83433	0	25	50	75	100
Roughness	132	160,5455	95,7039	21	78,25	149,5	220	368
Tension Strength	132	19,75758	9,202108	4	12	18,5	27	38
Elongation	132	1,625	0,762498	0,4	1,025	1,5	2,175	3,3

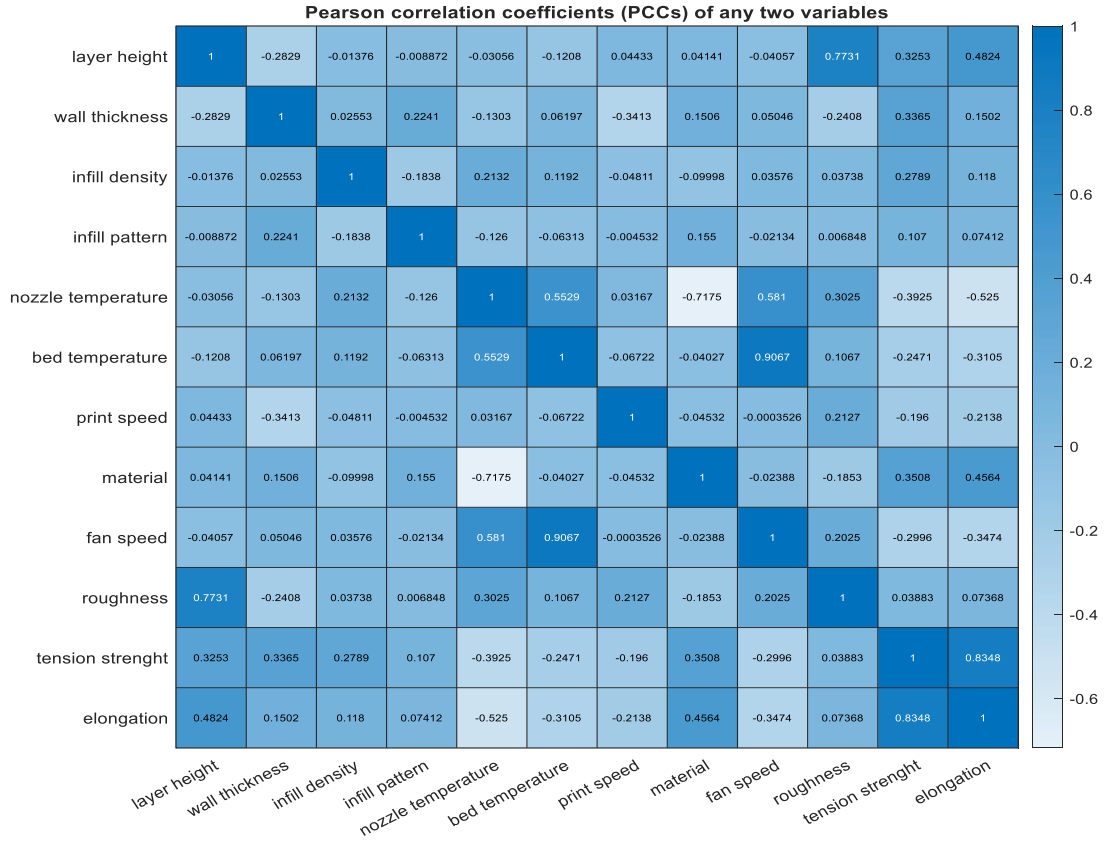

Figure 3. Coefficients of Pearson Correlation (PCC) of roughness, tension strength and elongation

Figure 3 presents the Pearson Correlation Coefficients (PCCs), which measure the strength and direction of linear relationships between pairs of variables. Upon analysis, it becomes evident that roughness, tensile strength, and elongation exhibit weak or insignificant linear correlations with other independent variables, such as layer height, wall thickness, infill density, nozzle temperature, bed temperature, print speed, and fan speed. This lack of strong linear associations suggests that these target variables may be influenced by more complex, non-linear interactions among the independent variables, which are not adequately captured through simple correlation metrics. The absence of significant linear relationships highlights the limitations of using basic statistical tools to understand the underlying patterns within the dataset. It indicates that the interactions between the variables are likely more intricate, requiring advanced methods to fully uncover and interpret their effects. For example, roughness may depend on a combination of layer height, print speed, and fan speed, but in a way that does not manifest as a straightforward linear relationship. Similarly, tensile strength and elongation could be affected by multiple features simultaneously, with interactions and thresholds that are not evident in linear analyses. In light of these findings, it became necessary to employ regression models capable of capturing complex, non-linear dependencies. To address this, three different machine learning models were developed as part of this study. These models aim to provide a more detailed understanding of the relationships between the independent variables and the target outputs. By leveraging machine learning techniques, the models are designed to identify hidden patterns, interactions, and trends that are not discernible using traditional linear approaches. This approach ensures a more robust and comprehensive analysis, offering valuable insights into the factors influencing roughness, tensile strength, and elongation, and ultimately supporting the optimization of 3D printing parameters for improved performance.

5.2. Single-variable partial dependence visualization for printed prototype of roughness, tension strength and elongation

Single-variable partial dependence plot is a type of plot that visualizes the effect of an independent variable on a target variable. This plot focuses on the analysis of only one independent variable and aims to isolate the effect of the selected variable on the target variable, holding the effect of all other independent variables constant. In this work, it has been used to increase the "explainability" of machine learning models (e.g., random forest, gradient boosting models) and understand how the model responds to that variable. In Figure 4, Figure 5 and Figure 6, the effect of 'layer height, wall thickness, infill density, infill pattern, nozzle temperature, bed temperature, print speed, material, fan speed on roughness, tension strenght and elongation are presented based on the result of partial dependency analysis.

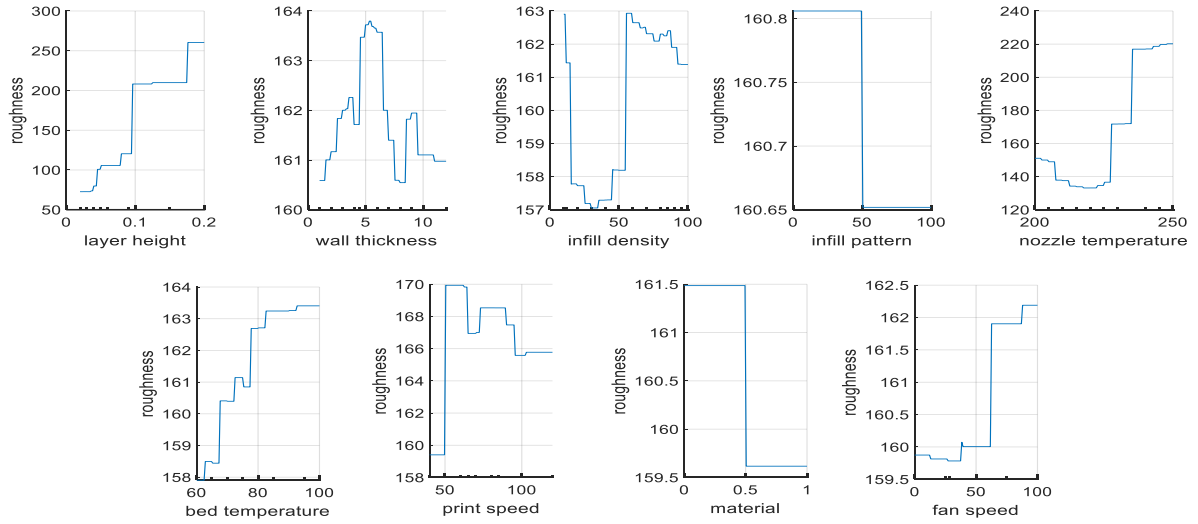

Figure 4. Single-variable partial dependence visualization for roughness

Figure 4 shows the effect of the specified parameters on roughness. When the graphs are considered, one of the most obvious changes is the increase in roughness as the layer height increases. In addition, an increase in roughness value is seen when the nozzle temperature exceeds 225°C.

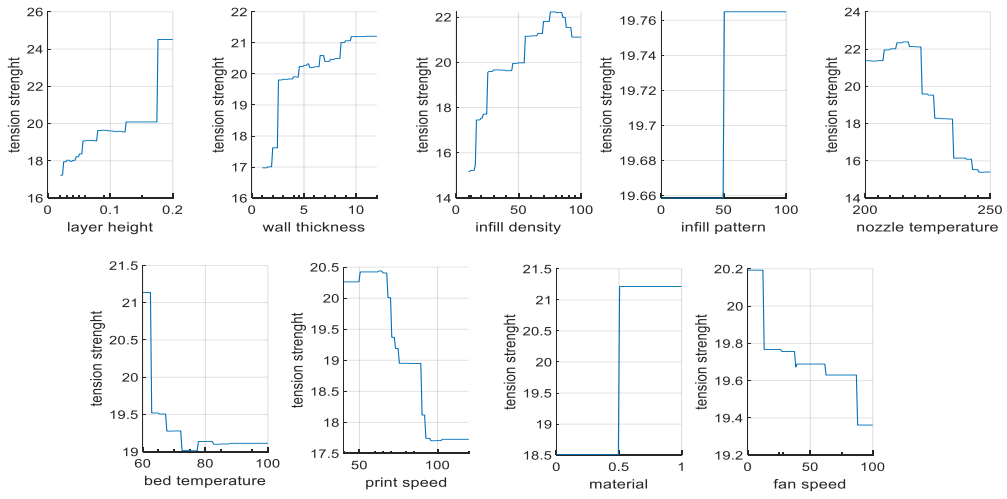

Figure 5. Single-variable partial dependence visualization for tension strenght

Figure 5 shows the effects of the input parameters on tension strength. The increase in fan speed, printing speed, nozzle temperature and bed temperature leads to a decrease in tension strength. It is seen that the optimum nozzle temperature is approximately 210 C and the optimum filling ratio is 90% for the specified conditions to obtain the highest tension strength. The increase in layer height and wall thickness also increases tension strength.

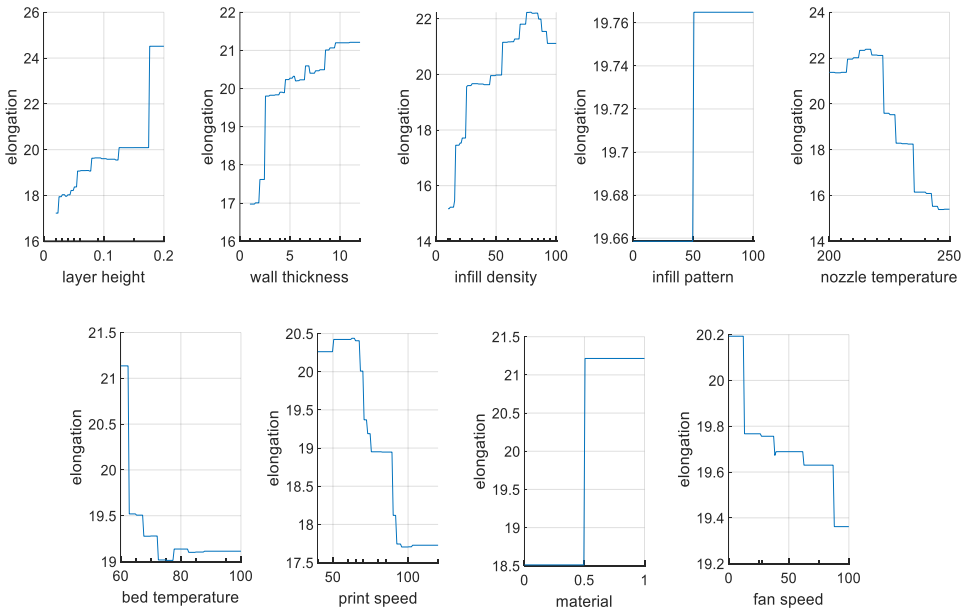

Figure 6. Single-variable partial dependence visualization for elongation

Figure 6 shows the results of the elongation effect according to these parameters. When the graphs are examined, it is seen that similar results are obtained to the effects seen in tension strength.

The success comparison of the methods according to the parameters of R^2, RMSE, MSE, MAE, estimation rate, training time is presented in Table 3.

Table 3. Performance metrics for *Elongation,Tension strength,Roughness* prediction

Parameter	Method	RMSE	R-Squared	MSE	MAE	Prediction Speed (obs/sec)	Training Time (sec)	Model Size (kB)
Elongation	MLR	0.51526	0.54	0.26549	0.40592	4900	5.9446	11
	DT	0.36187	0.77	0.13095	0.24103	2300	0.7988	9
	SVM	0.23887	0.90	0.057059	0.15823	2700	1.0253	10
	RF	0.30746	0.84	0.09453	0.21588	1600	2.4777	167
	GPR	0.10417	0.98	0.010852	0.027385	5400	1.0999	19
	MLP	0.2485	0.89	0.061754	0.062839	6200	2.0725	14
Tension strength	MLR	4.911	0.71	24.118	3.0868	1600	1.7326	53
	DT	5.3234	0.66	28.339	3.7534	4100	0.76664	8
	SVM	4.1156	0.80	16.938	2.6388	4100	0.67843	10
	RF	4.6571	0.74	21.688	3.0317	1700	2.0643	167
	GPR	2.833	0.90	8.0257	0.78883	5900	1.3456	19
	MLP	4.5639	0.75	20.829	1.5082	6700	3.1345	9
Roughness	MLR	51.458	0.71	2647.9	42.569	4000	1.1285	11
	DT	24.405	0.93	595.62	17.749	4700	1.4112	9
	SVM	10.745	0.99	115.46	9.8676	3600	0.80012	8
	RF	21.089	0.95	444.73	14.805	1200	4.7927	167
	GPR	1.3543	1.00	1.8341	0.24223	4200	2.3904	19
	MLP	4.8427	1.00	23.452	0.87258	6700	3.5984	9

According to Table 2, Gaussian Process Regression (GPR) emerges as the most accurate method overall. GPR consistently achieves the lowest error rates (RMSE, MSE, MAE) and the highest R^2 values across all parameters. For instance, in elongation, it achieves an RMSE of just 0.10417 and an R^2 of 0.98, demonstrating superior predictive performance. Similarly, in tension strength, GPR achieves an RMSE of 2.833 and an R^2 of 0.90, while in roughness, it reaches an RMSE of 1.3543 and an R^2 of 1.00, indicating exceptional accuracy. As alternatives, Support Vector Machine (SVM) and Artificial Neural Networks (MLP) also deliver commendable results in many cases. SVM, for example, performs well in predicting elongation and tension strength, with R^2 values of 0.90 and 0.80, respectively. MLP, on the other hand, matches GPR in terms of accuracy for roughness with an R^2 value of 1.00 while excelling in prediction speed. For instance, MLP achieves the fastest prediction speed at 6700 obs/sec. Meanwhile, Random Forest (RF) provides reasonably accurate results, though slightly less precise compared to GPR and SVM. RF's R^2values for elongation, tension strength, and roughness are 0.84, 0.74, and 0.95, respectively. However, its large model size (167 kB) and relatively slow prediction speed can be disadvantages in scenarios with large datasets. In contrast, Multiple Linear Regression (MLP) and Decision Tree (DT) methods generally perform worse in terms of accuracy compared to other methods. Linear Regression has the lowest performance in terms of RMSE and R^2. For example, in roughness, it records an RMSE of 51.458 and an R^2 of only 0.71. Similarly, DT offers faster prediction speeds but is limited in accuracy. So, Gaussian Process Regression (GPR) yielded the highest prediction accuracies: 0.98 for elongation, 0.90 for tensile strength, and 1.00 for roughness.

In conclusion, GPR is recommended for the highest accuracy and reliability, while MLP is ideal for speed-focused predictions. The combination of GPR's accuracy advantage and MLP's speed superiority highlights that the choice of method should depend on the requirements of the specific application. SVM offers a balanced option between accuracy and speed, whereas RF may face limitations in memory usage and prediction time with larger datasets.

Figure 7, Figure 8 and Figure 9 show the effect of the 3D printer's operating parameters, namely layer height, wall thickness, infill density, infill pattern, nozzle temperature, bed temperature, print speed, material, fan speed on the roughness, tension strength and elongation of the prototype part, which are predicted graphs in Figure 7. The predicted results of the MLR (a), DT (b), SVM (c), RF (d), GPR (e), MLP (f) models are presented with graphs, respectively. The x-axis represents the actual experimental data, and the y-axis represents the predicted values. The fact that the points are on the linear line shows the high success of the prediction.

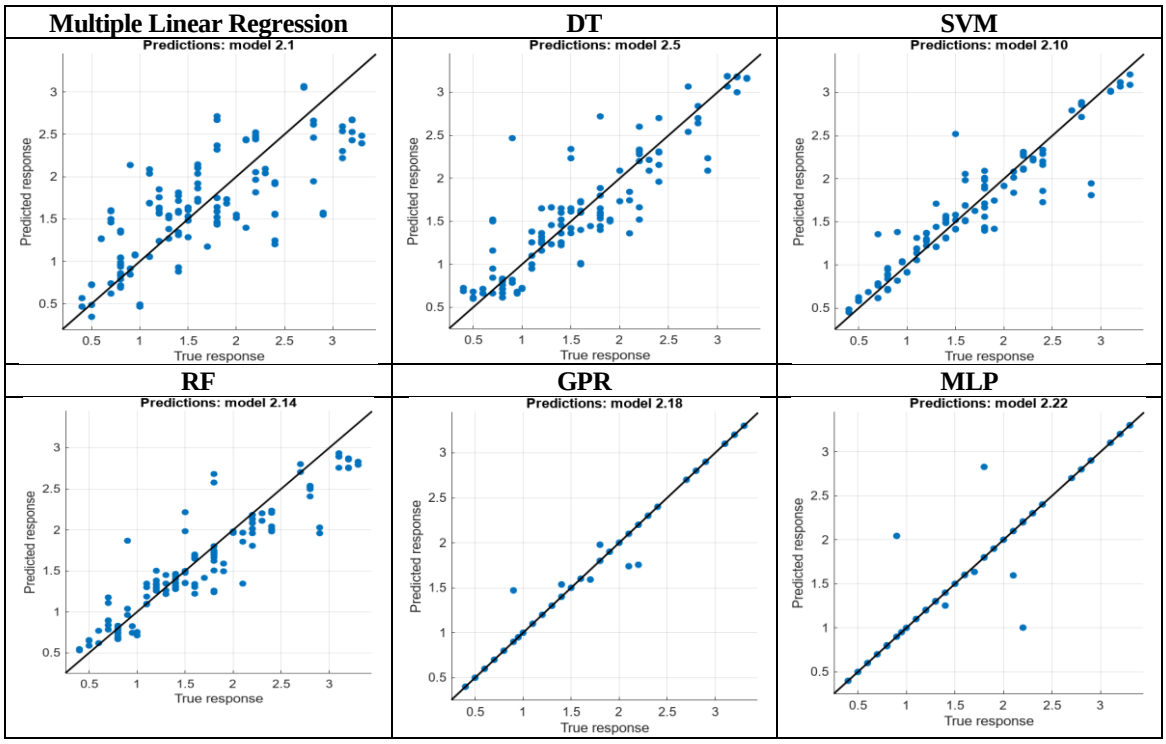

Figure 7. Prediction performance plots for elongation

Figure 7 shows the results of the prediction performance for elongation. According to the graphs, the most successful results are obtained with the GPR, SVM and MLP methods.

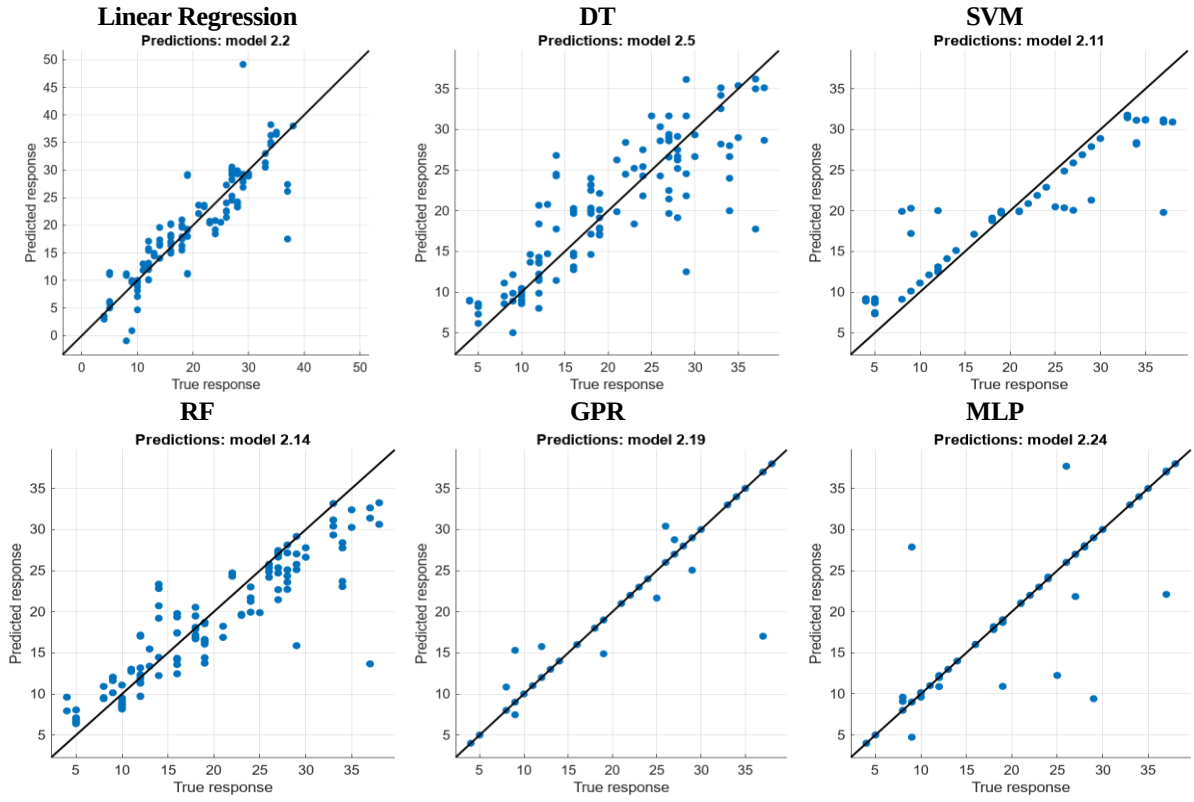

Figure 8. Prediction performance plots for tension strength

Figure 8 shows the results of the estimation performance for roughness. According to the graphs, the methods that make the estimation with maximum accuracy are GPR and MLP.

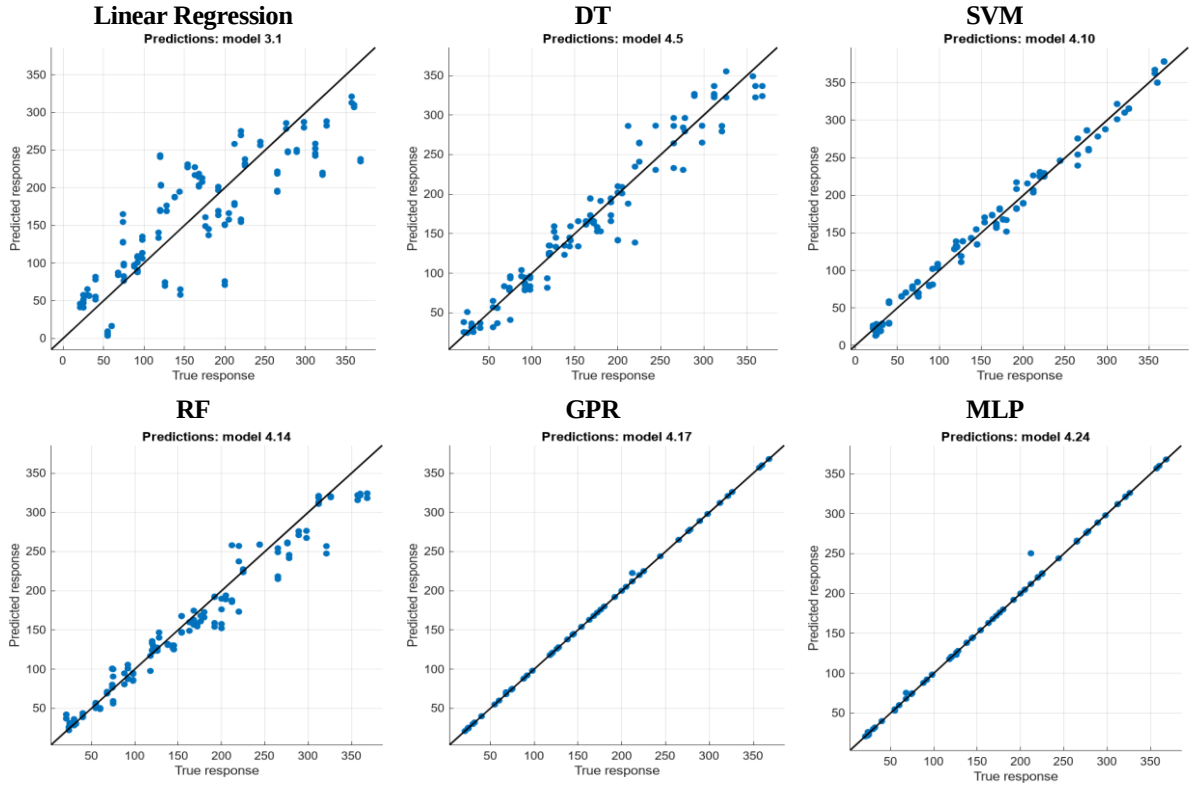

Figure 9. Prediction performance plots for roughness

In this study, only one work in the literature was identified that predicts the three performance metrics (elongation, tension strength, roughness) of parts produced using the same dataset. Table 4 was prepared to compare the results obtained using our methods with those reported by Nair et al. [27]. In their study, Nair and colleagues [27] utilized 29 different ML regression models and reported the lowest prediction errors for each output variable (elongation, roughness, tension Strength) based on Mean Absolute Error (MAE) values as follows: 0.3421 for the Elongation parameter using the Radial Basis Function Regression method, 39.2895 for the Roughness parameter using the Additive Regression method, and 5.2789 for the Tension Strength parameter using the Random Forest method.

In this study, the best prediction error values obtained for all three parameters were lower than those reported by Nair et al. Specifically, the prediction errors achieved in this study were 0.2485 for elongation (using the MLP method), 2.833 for tension strength (using the GPR method), and 1.3543 for roughness (using the GPR method).

Table 4. Performance comparison with studies using the same dataset

Parameter	Method	RMSE Value in [23]	RMSE Value in this study
Elongation	MLR	0.595	0.51526
	DT	0.732	0.36187
	SVM	-	0.23887
	RF	0.4908	0.30746
	GPR	-	0.10417
	MLP	0.5584	0.2485
Tension Strength	MLR	6.0349	4.911
	DT	11.3935	5.3234
	SVM	-	4.1156
	RF	5.8104	4.6571
	GPR	-	2.833
	MLP	10.0624	4.5639
Roughness	MLR	58.7044	51.458
	DT	68.348	24.405
	SVM	-	10.745
	RF	49.5023	21.089
	GPR	-	1.3543
	MLP	52.879	4.8427

6. Conclusion

In this study, a comprehensive machine learning-based analysis was conducted to evaluate the effects of various 3D printing parameters on the mechanical and aesthetic properties of printed outputs. Key parameters such as layer height, wall thickness, infill density, nozzle temperature, bed temperature, print speed, and fan speed were systematically varied, and their impacts on critical output characteristics, including surface roughness, tensile strength, and elongation, were assessed. The material type, particularly PLA and ABS, plays a crucial role in determining the roughness, tensile strength, and elongation of 3D-printed parts. PLA, known for its rigidity and ease of printing, typically produces smoother surfaces due to its lower melting temperature and better layer adhesion, resulting in reduced roughness. On the other hand, ABS exhibits higher elongation and better impact resistance due to its ductile nature, making it ideal for parts subjected to mechanical stresses. The choice between PLA and ABS thus directly influences the trade-offs between surface quality, strength, and flexibility, requiring careful consideration based on the intended application of the printed part.

The interplay between these parameters demonstrates the complex relationship between printing conditions and material performance, highlighting the need for fine-tuning to achieve a balance between surface quality, strength, and flexibility in 3D-printed parts.

The most successful methods in this study were estimation errors obtained using the MLP method for elongation, 0.2485, For tensile strength, it was obtained as 2.833 using the GPR method and for roughness, it was obtained as 1.3543 using the GPR method. This study demonstrates that machine learning models, particularly Gaussian Process Regression (GPR) and Multi-Layer Perceptron (MLP), provide highly accurate predictions of 3D-printed part quality. These findings highlight the potential for AI-driven optimization in additive manufacturing, reducing trial-and-error in material selection and print parameter adjustment.

7. Author Contribution Statement

The author processed the data. Interpreted the results and wrote manuscript.

8. Ethics Committee Approval and Conflict of Interest

There is no conflict of interest with any person/institution in the prepared article.

9. References

[1] J. Park, M. Chang, I. Jung, H. Lee, K. Cho, "3D Printing in the design and fabrication of anthromorphic hands: A review.", Adv. Intell. Syst., vol. 6, pp. 1-13, 2024.
[2] M. Sovetova, J. K. Calautit, "Influence of printing parameters on the thermal properties of 3D-printed construction structure", Energy, vol. 305, no. 132265, pp. 1-12, 2024.
[3] E. S. Chen, A. Ahmadianshalchi, S. S. Sparks, C. Chen, A. Deshwal, J. R. Doppa, K. Qiu, "Machine learning enabled design and optimization for 3D-Printing of high fidelity presurgical organ models", Adv. Mater. Technol., vol. 2400037, pp. 1-11, 2024.
[4] 3D Printer Material Requirement, URL: https://www.kaggle.com/datasets/shubhamgupta012/3d-printer-material-requirement/data.
[5] B. Taşar, A. Gülten, "EMG-Controlled Prosthetic hand with Fuzzy Logic Classification algorithm", vol. 321, pp. 321-341, 2017.
[6] O. Yaman, T. Tuncer, B. Taşar, "DES-Pat: A novel DES pattern-based propeller recognition method using underwater acoustical sounds", Appl. Acoust., vol. 175, no. 107859, pp. 1-13, 2021.
[7] A. K. Tanyıldızı, "Prototype design and manufacturing of a four-legged exploration robot with a three-dimensional (3D) printer", Int. J. 3D Print. Technol. Digit. Ind., vol. 7, no. 2, pp. 233-242, 2023.
[8] H. Ma, Y. Kou, H. Hu, Y. Wu, Z. Tang, "An investigate study on the oral health condition of individuals undergoing 3D-Printed customized dental implantation", J. Funct. Biomater., vol. 15, no. 156, pp. 1-12, 2024.
[9] F. Gorski, R. Wichniarek, W. Kuczko, M. Zukowska, "Study on properties of automatically designed 3D-printed customized prosthetic sockets", Mater., vol. 14, no. 18, 2021.
[10] M. van der Stelt, M. P. Grobusch, A. R. Koroma, M. Papenburg, I. Kebbie, C. H. Slump, T. J. J. Maal, L. Brouwers, "Pioneering low-cost 3D-printed transtibial prosthetics to serve a rural population in Sierra Leone – an observational cohort study", EClinicalMedicine, vol. 35, pp. 1-9, 2021.
[11] M. Mao, Z. Meng, X. Huang, H. Zhu, L. Wang, X. Tian, J. He, D. Li, B. Lu, "3D printing in space: from mechanical structures to living tissues", Int. J. Extreme Manuf., vol. 6, no. 023001, pp. 1-10, 2024.
[12] A. Zaman, J. Seo, "Design and control of autonomous flying excavator", Machines, vol. 12, no. 23, pp. 1-17, 2024.
[13] O. Doğan, M. S. Kamer, "Optimum spur gear design and production with additive manufacturing method", Bitlis Eren Univ. J. Sci., vol. 10, no. 3, pp. 1093-1103, 2021.
[14] M. Yang, C. Li, H. Liu, L. Huo, X. Yao, B. Wang, W. Yao, Z. Zhang, J. Ding, Y. Zhang, X. Ding, "Exploring the potential for carrying capacity and reusability of 3D printed concrete bridges: Construction, dismantlement and reconstruction of a box bridge", Case Stud. Constr. Mater., vol. 20, no. e02938, 2024.
[15] F. T. Omigdobun, N. O. Uwagboe, A. G. Udu, B. I. Oladapo, "Leveraging machine learning for optimized mechanical properties and 3D printing of PLA/cHAP for bone implant", Biomimetics, vol. 9, no. 587, pp. 1-23, 2024.
[16] M. Kasim, B. Owed, "The influence of infill density and speed of printing on the tensile properties of the three-dimension printing polylactic acid parts", J. Eng. Sustain. Dev., vol. 27, no. 1, pp. 95-103, 2023.
[17] Y. Zhang, K. Mao, S. Leigh, A. Shah, Z. Chao, G. Ma, "A parametric study of 3D printed polymer gears", Int. J. Adv. Manuf. Technol., vol. 107, pp. 4481-4492, 2020.
[18] R. J. R. Pereira, F. A. de Almeida, G. F. Gomes, "A multiobjective optimization parameters applied to additive manufacturing: DOE-based approach to 3D printing", Structures, vol. 55, pp. 1710-1731, 2023.
[19] A. R. Sani, A. Zolfagharian, A. Z. Kouzani, "Artificial Intelligence-augmented additive manufacturing: insights on closed-loop 3D printing", Adv. Intell. Syst., vol. 6, pp. 1-19, 2024.
[20] O. Sevli, "Prediction of the Material to be Used in 3D Printing with Machine Learning Techniques", Int. J. 3D Print. Technol. Digit. Ind., vol. 5, no. 3, pp. 596-605, 2021.
[21] S. R. Dabbagh, O. Ozcan, S. Tasoglu, "Machine learning-enabled optimization of extrusion-based 3D printing", Methods, vol. 206, pp. 27-40, 2022.

[22] V. S. Jatti, M. S. Sapre, A. V. Jatti, N. K. Khedkar, V. S. Jatti, "Mechanical properties of 3D-Printed components using fused deposition modeling: optimization using the desirability approach and machine learning regressor", Appl. Syst. Innov., vol. 5, no. 112, pp. 1-15, 2022.
[23] N. Çelik, S. Kapan, B. Taşar, "Effects of various parameters on entropy generation and exergy destruction in a coil wire inserted heat exchanger by using deep learning neural network method", Int. Commun. Heat Mass Transf., vol. 161, no. 108481, 2025.
[24] N. Çelik, B. Taşar, S. Kapan, "Performance optimization of a heat exchanger with coiled-wire turbulator insert by using various machine learning methods", Int. J. Therm. Sci., vol. 192, no. 108439, 2023.
[25] M. Li, S. Yin, Z. Liu, H. Zhang, "Machine learning enables electrical resistivity modeling of printed lines in aerosol jet 3D printing", Sci. Rep., vol. 14, no. 1, 2024.
[26] M. R. Ebers, K. M. Steele, J. N. Kutz, "Discrepancy Modeling Framework: Learning missing physics, modeling systematic residuals, and disambiguating between deterministic and random effects", arXiv:2203.05164v2 [stat.ML], 2023.
[27] A. Nair, J. Jebakumar, K. Raj, "Machine learning model selection for performance prediction in 3D printing", J. Inst. Eng. India Ser. C, vol. 103, no. 4, pp. 847-855, 2022.